

Cite this: *Nanoscale*, 2018, **10**, 1180

Graphene oxide is degraded by neutrophils and the degradation products are non-genotoxic†

Sourav P. Mukherjee,^a Anda R. Gliga,^a Beatrice Lazzaretto,^a Birgit Brandner,^b Matthew Fielden,^c Carmen Vogt,^c Leon Newman,^d Artur F. Rodrigues,^d Wenting Shao,^e Philip M. Fournier,^e Muhammet S. Toprak,^{id}^c Alexander Star,^{id}^e Kostas Kostarelos,^d Kunal Bhattacharya^a and Bengt Fadeel^{id}^{*a}

Neutrophils were previously shown to digest oxidized carbon nanotubes through a myeloperoxidase (MPO)-dependent mechanism, and graphene oxide (GO) was found to undergo degradation when incubated with purified MPO, but there are no studies to date showing degradation of GO by neutrophils. Here we produced endotoxin-free GO by a modified Hummers' method and asked whether primary human neutrophils stimulated to produce neutrophil extracellular traps or activated to undergo degranulation are capable of digesting GO. Biodegradation was assessed using a range of techniques including Raman spectroscopy, transmission electron microscopy, atomic force microscopy, and mass spectrometry. GO sheets of differing lateral dimensions were effectively degraded by neutrophils. As the degradation products could have toxicological implications, we also evaluated the impact of degraded GO on the bronchial epithelial cell line BEAS-2B. MPO-degraded GO was found to be non-cytotoxic and did not elicit any DNA damage. Taken together, these studies have shown that neutrophils can digest GO and that the biodegraded GO is non-toxic for human lung cells.

Received 18th May 2017,
 Accepted 16th December 2017
 DOI: 10.1039/c7nr03552g
rsc.li/nanoscale

Introduction

Graphene and its derivatives have attracted tremendous attention for various applications in science and technology.¹ Graphene oxide (GO), in particular, is being intensively investigated for various biomedical applications including drug delivery and bioimaging, and as biosensors.² GO offers interesting physicochemical properties including its large surface area, ease of surface functionalization, and enhanced colloidal stability in aqueous media when compared to pristine graphene.³ However, increasing production and use of graphene-based materials also necessitates careful scrutiny of the impact of such materials on human cells and tissues. Understanding the interaction of novel materials with cells of the innate immune system is of particular importance.⁴ Once inside the

body, a foreign material will encounter phagocytic cells of the immune system, such as neutrophils, macrophages, or dendritic cells. These cells represent the first line of defense against foreign intrusion (microorganisms, particles) and they also clear cell debris. Neutrophils employ three strategies to eliminate invading microbes: (1) microbial uptake followed by intracellular destruction through an array of proteolytic and oxidative enzymes, (2) degranulation and secretion of antimicrobial factors such as myeloperoxidase (MPO) leading to extracellular destruction of microbes, and (3) release of neutrophil extracellular traps (NETs) with entrapment and non-phagocytic killing of microbes.^{5,6} NETs consist of a network of chromatin fibers decorated with antimicrobial proteins and oxidative enzymes such as neutrophil elastase (NE) and MPO to enable the extracellular killing of bacteria or fungi.⁷ MPO, which is abundantly expressed in cytoplasmic granules, and is also present in NETs, catalyzes the production of hypochlorous acid (HOCl) from hydrogen peroxide (H₂O₂) and chloride anion (Cl⁻).⁸ In addition to its role in host defense against pathogens, MPO has been reported capable of degrading carbon-based nanomaterials.² MPO-mediated destruction of oxidized single-walled carbon nanotubes (SWCNTs) was first described by Kagan *et al.*⁹ The biodegraded nanotubes did not generate an inflammatory response when aspirated into the lungs of mice. Moreover, clearance of SWCNTs from the lungs of MPO-deficient mice was markedly less effective whereas the

^aNanosafety & Nanomedicine Laboratory, Division of Molecular Toxicology, Institute of Environmental Medicine, Karolinska Institutet, Stockholm, Sweden.
 E-mail: bengt.fadeel@ki.se; Tel: +46 8 524 877 37

^bUnit for Chemistry, Materials and Surfaces, SP Technical Research Institute of Sweden, Stockholm, Sweden

^cDepartment of Applied Physics, School of Engineering Sciences, Royal Institute of Technology, Stockholm, Sweden

^dNanomedicine Laboratory, Faculty of Medical & Human Sciences and National Graphene Institute, University of Manchester, Manchester, UK

^eDepartment of Chemistry, University of Pittsburgh, Pittsburgh, PA, USA

† Electronic supplementary information (ESI) available. See DOI: [10.1039/c7nr03552g](https://doi.org/10.1039/c7nr03552g)

inflammatory response was more pronounced than in wild-type mice.¹⁰ Subsequent studies showed that NETs from *ex vivo* activated human neutrophils can trap and digest SWCNTs through an MPO-dependent mechanism.¹¹ More recently, Kurapati *et al.*¹² reported that purified MPO can digest highly dispersed GO sheets in the presence of H₂O₂, while aggregated GO sheets failed to undergo degradation. Others reported, based on the determination of characteristic Raman signatures, that carboxylated graphene is present in lung, liver, kidney and spleen of mice after intravenous injection with a gradual development of structural disorder over a period of 3 months.¹³ This suggested that some degradation of graphene could occur *in vivo* although the actual mechanism remained elusive. In fact, studies on the enzymatic degradation of graphene or its derivatives by immune cells are currently lacking. Moreover, there are no studies on the potential impact of the degradation products. It is important to note that incomplete degradation of SWCNTs by peroxidases results in the formation of different oxidized aromatic hydrocarbons, which are potentially genotoxic.¹⁴ In addition, Bai *et al.*¹⁵ suggested that degradation of GO *via* the photo-Fenton reaction could yield oxidized polycyclic aromatic hydrocarbon intermediates. Pan *et al.*¹⁶ found that extracts from SWCNTs subjected to peroxidase degradation for 5 to 10 days could trigger DNA damage in lung carcinoma cells. Here we synthesized GO and assessed whether it is degraded by neutrophils and whether this is MPO-dependent, using activated, degranulating neutrophils, or purified NETs. We also studied the degradation of GO using recombinant MPO, and determined whether MPO-degraded GO of different lateral sizes was cytotoxic or genotoxic using transformed, non-tumorigenic human bronchial epithelial cells (BEAS-2B).

Experimental section

Reagents

Recombinant human myeloperoxidase was purchased from Planta Natural Products (Vienna, Austria). Myeloperoxidase inhibitor-1 was purchased from Santa Cruz Biotechnology (USA). Penicillin-streptomycin, L-glutamine and phosphate buffer saline (PBS) were from Gibco Invitrogen (Sweden). Dextran (MW 150 000), phorbol 12-myristate 13-acetate (PMA), f-Met-Leu-Phe (fMLP), hydrogen peroxide (H₂O₂), sodium chloride (NaCl), catalase (from bovine liver), cytochalasin B, bovine serum albumin (BSA), were purchased from Sigma Aldrich (Sweden). Lymphoprep was from Axis Shield (Oslo, Norway). Alamar Blue dye was purchased from Thermo Scientific (Sweden). BEGM™ Bronchial Epithelial Cell Growth Medium and BEGM™ BulletKit™ were purchased from Lonza (BioNordika AB, Sweden). Trevigen comet microscope slides and Trevigen comet lysis solution were purchased from Nordic BioSite AB (Sweden). Benzo[a]pyrene was provided by Kristian Dreij, Institute of Environmental Medicine, Karolinska Institutet (Sweden).

GO synthesis and characterization

Graphene oxide (GO) sheets of differing lateral dimensions were synthesized using the modified Hummers' method as

previously described¹⁷ under endotoxin-free conditions by using a laminar flow hood, water for injection, gloves, non-pyrogenic plastic containers and depyrogenated glassware.¹⁸ The structural properties such as lateral dimension and thickness of the GO sheets were studied by optical microscopy, transmission electron microscopy (TEM) and atomic force microscopy (AFM) and detailed results are reported elsewhere.¹⁹ In brief, samples were prepared by drop-casting the GO materials onto a freshly cleaved mica surface coated with 0.01% poly-L-lysine (Sigma). After washing off excess material and allowing the samples to dry overnight, AFM images were acquired using a Bruker Multimode 8 AFM in tapping mode with an OTESPA probe (Bruker, nominal $f_0 = 300$ kHz, $k = 42$ N m⁻¹). For TEM analysis, 10 µL of the GO samples were deposited onto a glow discharged carbon-coated copper grid (CF400-Cu) and filter paper was used to remove any excess material after 1 min of deposition time. The samples were then observed with a FEI Tecnai 12 BioTWIN microscope at an acceleration voltage of 100 kV and images were taken with a Gatan Orius SC1000 CCD camera. Furthermore, the endotoxin content in the GO samples was assessed using the TNF-α expression test (TET), as previously described and both GO-S and GO-L were shown to be endotoxin-free.¹⁸

Degradation by human myeloperoxidase

Mixtures containing 5 µg MPO (Planta Natural Products, Vienna, Austria) per 50 µg of GO sample (final concentration 100 µg mL⁻¹) and large (GO-L) or small sheets (GO-S) were suspended in 500 µL of autoclaved Milli-Q water containing 140 mM NaCl in the presence or absence of myeloperoxidase inhibitor-1. Hydrogen peroxide was added at a rate of 100 µM h⁻¹ for 12 h. The pH of the suspensions was acidified from pH 7.4 to approx. 6 upon repeated addition of H₂O₂ (data not shown), but this is nevertheless compatible with peroxidase activity and also comparable to the pH range within neutrophil phagosomes.⁸ The MPO enzyme was replenished after 6 h and the reaction mixture was maintained at 37 °C. Just after initiation of the experiment (0 h) and after 6 h and 12 h, the reactions were stopped by freezing the samples and samples were stored at -20 °C for further analyses.

Neutrophil isolation and degranulation

Neutrophils were isolated from buffy coat of healthy human blood donors (Karolinska University Hospital, Stockholm, Sweden) as previously described.²⁰ Briefly, neutrophils were separated by density gradient centrifugation using Lymphoprep (Axis Shield, Oslo, Norway) followed by gradient sedimentation in a 5% dextran solution and hypotonic lysis of residual erythrocytes. Isolated polymorphonuclear neutrophils (PMNs) were maintained in phenol red-free RPMI 1640 culture medium (Sigma) supplemented with 2 mM L-glutamine, 100 U mL⁻¹ penicillin and 100 mg mL⁻¹ streptomycin without serum in 5% CO₂ at 37 °C and incubated with GO-S or G-L (100 µg mL⁻¹) in the presence of fMLP (10 nM) and cytochalasin B (5 µg mL⁻¹) for 3 h and 6 h, to trigger degranulation.²¹ After the indicated time-points of exposure the samples were

collected, centrifuged at 1000 rpm for 10 min and the supernatant which contained the GO sheets (along with cell debris) was transferred to a fresh tube and stored at -80 °C for analysis by Raman microspectroscopy.

Neutrophil extracellular trap induction

PMNs were freshly isolated from buffy coats of healthy human blood donors as described above. After isolation, the PMNs were immediately stimulated with 25 nM PMA for 3 h at 37 °C to trigger production of neutrophil extracellular traps (NETs). Then, NETs were collected from the exposure medium as described²² and incubated with GO-L (100 µg mL⁻¹) up to 12 h in a NaCl solution (140 mM) in the presence or absence of myeloperoxidase inhibitor-1 (600 nM) with addition of H₂O₂ (25 µM) every hour. After 6 h and 12 h incubation with purified NETs, GO degradation was analyzed by confocal Raman microspectroscopy.

Confocal Raman microspectroscopy

GO-S or GO-L incubated as specified above with recombinant MPO or with degranulating cells, or with purified NETs, were drop-casted onto a quartz slide and dried. Raman analysis was performed as previously described²³ using a confocal Raman microspectroscopy (WITec alpha300 system, Germany) with a laser of 532 nm wavelength set at an integration time of 0.5 s and 600× magnification. The scan area for each sample was adjusted to 100 × 100 µm and 3 areas were analyzed per sample. For determination of the D-band (asymmetric mode peak, 1354 cm⁻¹) and G-band (tangential C-C stretching modes, 1582 cm⁻¹), an average of the whole scan (*i.e.*, 10 000 spectra per sample) was calculated and displayed. D : G ratios were also calculated and displayed.¹²

Transmission electron microscopy

GO-S and GO-L were analyzed using transmission electron microscopy (TEM) (JEM-2100F, 200 kV, JEOL). The dialysed suspension of GO sheets before and after 12 h digestion was dispensed on the TEM grid and air dried for 24 h prior analysis. Both GO-S and GO-L were dialysed after the biodegradation experiment using Mini Dialysis Kit (1 kDa) from Sigma-Aldrich following the manufacturer's instruction. Briefly, 250 µL of each sample were added in dialysis tubes. Dialysis tubes were placed inverted into a beaker containing 2 L of Milli-Q® water and dialyzed while stirring (300 rpm) at 30 °C. After 6 h, the Milli-Q® water was replaced with 2 L of fresh Milli-Q® water and the dialysis continued (while stirring) overnight at room temperature. Then, samples were collected in the tube by brief centrifugation (30 s at 4000 rpm) and the dialysis cap was replaced with a normal cap (without membrane) provided with the kit. The samples were then used for TEM and AFM.

Atomic force microscopy

GO-L flakes incubated for 6 h or 12 h with recombinant MPO + NaCl + H₂O₂, were dialysed as above, spin coated on a clean mica sheet and AFM measurements were performed under a

nitrogen atmosphere with a TESPA probe (Bruker, nominal $f_0 = 300$ kHz, $k = 40$ N m⁻¹) using a Bruker Dimension Icon AFM. The images were acquired at 1 Hz in tapping mode.

MALDI-TOF mass spectrometry

Matrix-assisted laser desorption/ionization time-of-flight mass spectrometry (MALDI-TOF MS) was used to study the biodegradation of the small GO sheets (GO-S) upon incubation with MPO in the presence of NaCl and H₂O₂, as described above. A Voyager-DE PRO MALDI TOF mass spectrometer (AB Sciex, Framingham, MA) was utilized for laser desorption/ionization (LDI) data. Filtered/lyophilized GO-S samples subjected to degradation for the indicated time-points were resuspended in Milli-Q water at a concentration of 0.1 mg mL⁻¹ and tested without any matrix. To this end, 5 µL of sample solution was dropped onto a MALDI plate and dried under ambient conditions. For data acquisition, the instrument settings were positive reflector mode; 20 000 V accelerating voltage, grid voltage equals 75% accelerating voltage, 1.12 mirror to accelerating voltage ratio, 180 ns extraction delay, and 1500 laser intensity with N₂ laser source. Peaks spaced by 12 Da across the spectrum of mass-to-charge ratios correspond to carbon atoms from GO.

BEAS-2B lung cell culture

The human SV40-transformed lung cell line BEAS-2B (European Collection of Cell Cultures) was cultured in bronchial epithelial cell growth medium (BEGM, Lonza) supplemented with BEGM bullet-kit (recombinant epidermal growth factor (EGF), hydrocortisone, insulin, bovine pituitary extract, GA-1000 (gentamicin sulfate and amphotericin-B), retinoic acid, transferrin, triiodothyronine and epinephrine) (Lonza). Cells were cultured in flasks and plates pre-coated with: 0.01 mg mL⁻¹ fibronectin, 0.03 mg mL⁻¹ bovine collagen type I, 0.01 mg mL⁻¹ bovine serum albumin and 0.2% penicillin-streptomycin in BEGM additive free medium for 2 h prior to seeding. Cells were maintained in a humidified atmosphere at 37 °C, 5% CO₂ and subcultured at 80% confluence.

Cytotoxicity and genotoxicity assessment

GO-L and GO-S sheets were oxidatively biodegraded by MPO in the presence of NaCl and H₂O₂ for the indicated time-points following the procedure mentioned above. To reduce the excess H₂O₂, the reaction mixture was then treated for 1 h at 37 °C with 2250 units of bovine liver catalase, where 1 unit of catalase can decompose 1 µM H₂O₂ per min at pH = 7, according to the manufacturer's instruction (Sigma-Aldrich). For cytotoxicity and genotoxicity assessment, BEAS-2B cells were seeded in 96-well plates (1 × 10⁵ cells per mL, 100 µL cell medium per well). Then, cells were exposed for 24 h to the GO-L or GO-S biodegradation reaction mixtures diluted in the BEGM complete medium to an equivalent of 0, 12.5, 25 and 50 µg mL⁻¹ concentrations of intact GO-L and GO-S. *Alamar Blue* (AB) assay was performed for cytotoxicity assessment of the biodegradation samples. DMSO (5%) was used as a positive control. Benzo[a]pyrene (B[a]P) at 10, 100 and 200 µM con-

centrations were also tested in parallel, along with 25 $\mu\text{g mL}^{-1}$ GO-L and GO-S mixed with 200 μM B[a]P. After the exposure period the AB assay was performed according to the manufacturer's instruction. Briefly, medium was removed, cells were rinsed with PBS and 100 μL of AB medium (5% [v/v] solution of AlamarBlue® reagent) prepared freshly in the BEGM complete medium were added to each well. After 2 h of incubation at 37 °C, fluorescence was measured at the respective excitation and emission wavelength of 531 nm and 595 nm using a Tecan Infinite F200 plate reader. AB solution in the BEGM complete medium alone was included as blank. The experiment was performed with at least three biological replicates and three technical replicates for each concentration of GO. Results were expressed as percentage cell viability *versus* control. To control for interference,²⁴ the GO degradation reaction mixture was maintained in cell-free medium and mixed with the AB dye; no interference was observed (data not shown). *Alkaline comet assay* was performed on the BEAS-2B cells to measure the DNA damage or genotoxicity of the GO-L and GO-S biodegradation reaction mixtures diluted in the BEGM complete medium at an equivalent of 0, 12.5 and 25 $\mu\text{g mL}^{-1}$ concentrations of GO-L and GO-S. BEAS-2B cells were exposed for 24 h and cells were then washed and harvested using trypsin and re-suspended in PBS. Ten μL cell suspensions were mixed with 60 μL 1% low-melting point agarose (Sigma-Aldrich) at 37 °C and 40 μL of this mixture were then placed on microscope slides (Trevigen). The slides were then placed in lysis solution (Trevigen) for 1 h on ice in the dark and transferred to electrophoresis buffer (0.3 M NaOH, 1 mM EDTA, pH > 13) for 40 min on ice in the dark for the DNA unwinding, followed by electrophoresis (29 V) in the same buffer for 30 min. Slides were neutralized in 0.4 M Tris buffer 2 × 5 min, rinsed in deionized water for 5 min and fixed with methanol for 5 min. DNA was stained for 30 min in 1 : 10 000 SYBR-green solution (Sigma-Aldrich) prepared in TAE buffer (Sigma-Aldrich). Comet scoring was performed on a fluorescence microscope (Leica DMLB) equipped with comet assay IV software (Perceptive Instruments). At least 50 nucleoids were scored per gel with duplicate gels for each sample (total of 100 nucleoids per sample); triplicate samples were prepared for each exposure. H₂O₂ (5 min, 50 μM) and benzo[a]pyrene (24 h, 200 μM) was used as positive controls. Additional controls included B[a]P + GO-S or GO-L (25 $\mu\text{g mL}^{-1}$) and H₂O₂ + catalase. The results are expressed as % DNA in tail and presented as mean values ± S.D.

Results and discussion

Synthesis of endotoxin-free graphene oxide

GO sheets were synthesized using the modified Hummers' method as previously described.¹⁷ The synthesis was performed under endotoxin-free conditions and the materials were found to be endotoxin-free (data not shown) which is important for studies using immune cells. Indeed, it has been demonstrated that neutrophils release NETs in the presence of

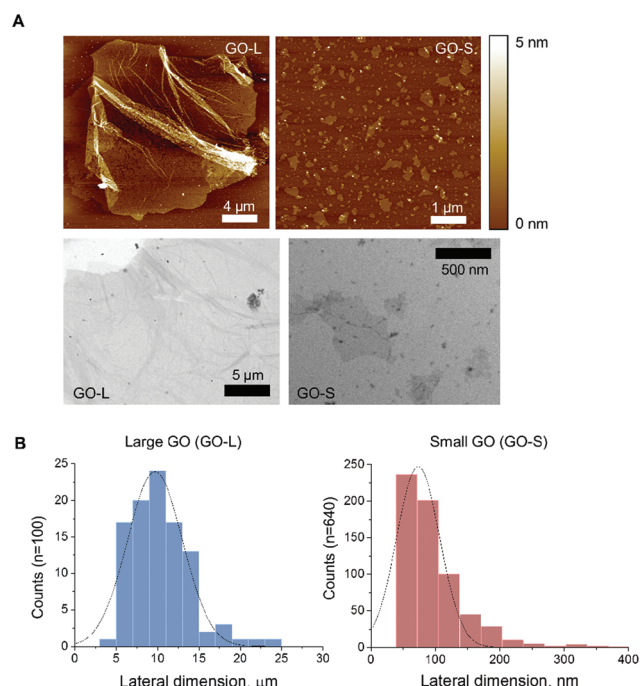


Fig. 1 Characterization of graphene oxide samples. (a) Representative TEM and AFM images of GO-L and GO-S. (b) Lateral dimension distribution analysis of GO-L and GO-S.

only a few picograms of bacterial LPS per cell.²⁵ Structural characterization using TEM and AFM is shown in Fig. 1A. The lateral dimensions of small (GO-S) and large (GO-L) sheets were 100 ± 50 nm and 10 ± 8 μm , respectively (Fig. 1B).

Degradation of GO by recombinant MPO

We initially studied the biodegradation of GO-L by recombinant human MPO, using established protocols.⁹ Degradation appeared to be almost complete after 12 h of incubation as evidenced by the translucent appearance of the suspensions (Fig. 2A). To ensure that the degradation was not merely a result of chemical degradation by H₂O₂, we included samples with H₂O₂ (without MPO) and samples with MPO (without H₂O₂). Degradation was seen only in the presence of the full system (MPO + H₂O₂ + NaCl) (Fig. 2A). Based on previous degradation studies of CNTs, it is presumed that the synergistic effects of HOCl and reactive intermediates formed by MPO may explain the higher efficiency of degradation of the MPO + H₂O₂ + NaCl system *versus* the HRP + H₂O₂ system.²⁶

To verify that biodegradation occurred, we utilized confocal Raman microspectroscopic mapping of the samples following incubation for 0 h, 6 h, and 12 h with the complete system (*i.e.*, MPO + H₂O₂ + NaCl). Raman confocal mapping enabled the collection and analysis of 10 000 spectra per sample (per scan area). At 6 h, a slight decrease in the intensity of the characteristic broad D band (1354 cm^{-1}) and G band (1582 cm^{-1}) of GO was noted while the D and G bands were strongly diminished after 12 h confirming the complete degradation of the GO sheets (Fig. 2B). By comparison, in a study by

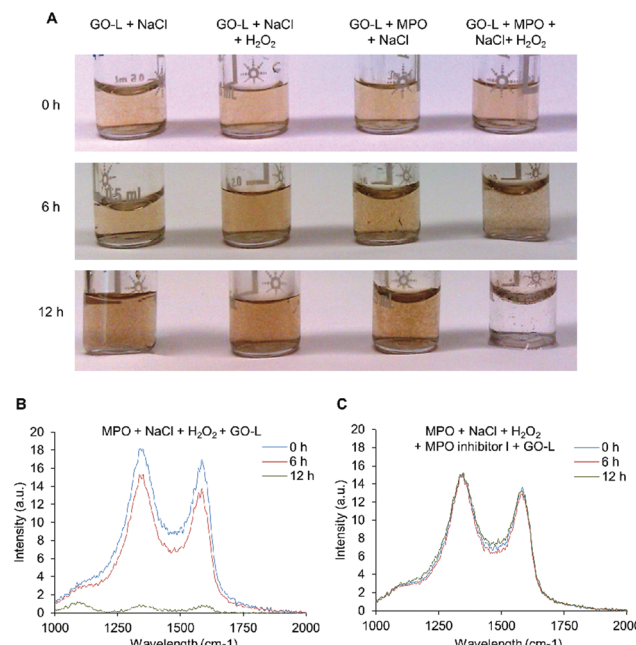


Fig. 2 MPO-mediated degradation of GO. (a) Photographs of the reaction vials containing GO-L after 0–12 h of incubation in the presence of NaCl, NaCl + H₂O₂, MPO + NaCl, and MPO + NaCl + H₂O₂, respectively. GO incubated with the complete reaction mixture clearly showed almost complete degradation of GO-L sheets after 12 h incubation. (b) Raman confocal microspectroscopic analysis of GO-L samples after incubation with MPO + NaCl + H₂O₂ for 0, 6, and 12 h showed almost complete degradation of GO, as evidenced by the suppression of the characteristic D band (1354 cm^{-1}) and G band (1582 cm^{-1}), while no degradation of GO-L was seen in the presence of MPO inhibitor-1 (0.6 μM) (c). The data shown represent an average of the whole scan (10 000 spectra per sample).

Kurapati *et al.*¹² partial degradation of GO was seen at 15 h and complete degradation was seen after 24 h of incubation with MPO, based on Raman spectroscopic analysis. However, averages of only 5 spectra were shown in the latter study whereas confocal mapping enables a more extensive coverage of the sample. When we incubated GO with MPO + H₂O₂ + NaCl in the presence of myeloperoxidase inhibitor-1, the D and G bands were maintained (Fig. 2C), thus confirming that degradation was MPO-mediated in this system.

We also asked whether small GO sheets were degraded by MPO. To this end, we incubated GO-S or GO-L with the full degradation system (*i.e.*, MPO + H₂O₂ + NaCl) for 0 h or 12 h and visualized the suspensions (Fig. 3A). In addition, confocal Raman microspectroscopic mapping of the samples was performed at 0 h, 6 h, 9 h, and 12 h, and the D : G intensity ratio was determined (Fig. 3B). The intensity ratio provides information about the disorder in the graphitic lattice of the GO sheets,¹² and our results showed that the ratio increased with incubation time indicating an increase in the defect sites in the structure. Next, we performed TEM analysis of GO sheets incubated with MPO + H₂O₂ + NaCl for 12 h. The characteristic shape and morphology of the GO sheets disappeared, with evidence of perforations and degradation into smaller fragments

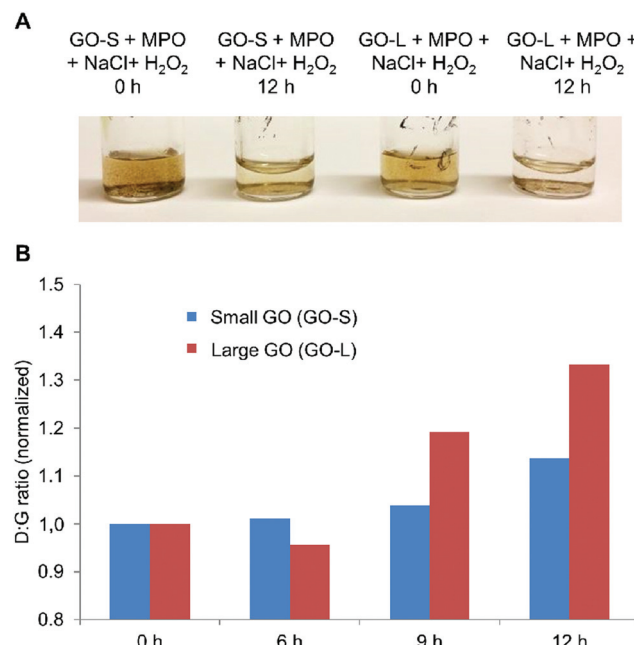


Fig. 3 Biodegradation of small versus large GO. (a) Photographs of the reaction vials containing GO-S and GO-L at 0 h and 12 h of incubation in the presence of MPO + NaCl + H₂O₂. (b) Raman analysis of GO-S and GO-L incubated as in (a). The D : G ratios increased with incubation time indicating increases in the number of defect sites in the graphitic lattice of the GO sheets. The data represent an average of 10 000 spectra per sample.

(Fig. 4A–C) as compared to the parental sample (Fig. 4D–F), thus supporting the results of the Raman spectroscopy. We also conducted AFM imaging of GO sheets to monitor for any holes or defects formed in the basal plane. AFM imaging of GO-L just after the addition of MPO + H₂O₂ + NaCl (*i.e.*, 0 h) showed the attachment of MPO on the surface of the GO sheet (Fig. 4G). This is expected as MPO is a highly cationic protein and is known to attach to negatively charged surfaces.¹² Notably, the formation of significant defects was evident after a 6 h incubation with MPO (Fig. 4H). Further AFM studies of GO-L (ESI Fig. 1A–D†) and GO-S (ESI Fig. 1E–F†) incubated with or without MPO + H₂O₂ + NaCl disclosed remarkable changes in both GO samples at 12 h. These features resembled the holes formed after interaction of GO with horseradish peroxidase (HRP) for 10 days,²⁷ but MPO-mediated degradation of GO occurred more rapidly.

GO biodegradation by degranulating neutrophils

Previous work has demonstrated that neutrophils are capable of enzymatic degradation of SWCNTs, and opsonization with immunoglobulins was shown to enhance the cellular uptake of the nanomaterials.⁹ However, neutrophils may also execute their degradative functions extracellularly. Hence, degranulation of neutrophils leads to the secretion of granule proteins which are present in at least three distinct granule populations, *i.e.*, primary or azurophil granules, secondary or specific granules, and tertiary granules, and from secretory

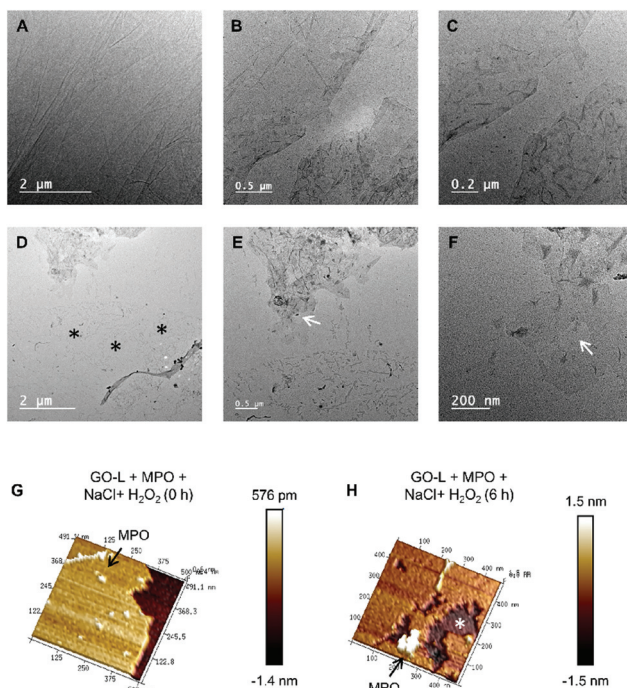


Fig. 4 TEM and AFM analysis of GO degradation. TEM images of GO-S before (a–c) and after 12 h (d–f) of acellular biodegradation in the presence of MPO + NaCl + H₂O₂. The arrows point to holes formed in the GO sheets and asterisks show small biodegraded flakes/fragments. (g–h) AFM imaging of GO-L samples incubated for 0 h and 6 h with recombinant MPO in the presence of NaCl + H₂O₂ showed the formation of holes in the basal plane. Arrows indicate adsorbed MPO protein and the asterisk marks a defect in GO-L.

vesicles.^{28,29} The primary granules contain MPO, NE, and other bactericidal factors. The N-formylated tripeptide, fMLP (*N*-formyl-methionyl-leucyl-phenylalanine) is a potent activator of neutrophils³⁰ and cytochalasin B (CB) enhances several fMLP-stimulated neutrophil responses, including aggregation, superoxide production, and degranulation.³¹ In this study, freshly isolated primary human neutrophils were activated with fMLP + CB and incubated with GO-S and GO-L for 3 h or 6 h. Exogenous H₂O₂ was not added, as the activated neutrophil already contains the complete system required for degradation (of microbes).⁸ Thereafter, biodegradation of the GO sheets was analyzed by confocal Raman microspectrometric mapping. GO-S was significantly degraded at 3 h and 6 h, as indicated by the reduction in the D and G band intensities (Fig. 5A). For GO-L, the D and G band intensities were diminished at 3 h and significantly suppressed at 6 h (Fig. 5B). Overall, these results showed that primary human neutrophils can degrade GO extracellularly and that degradation of GO is rapid, but also that GO-S (approx. 100 nm) biodegraded at a faster rate than GO-L (approx. 10 μm).

Cell-free GO degradation in neutrophil extracellular traps

Neutrophils produce so-called NETs to capture bacteria or other microorganisms.⁵ Previous studies demonstrated that enzymatically active MPO is present in NETs; however,

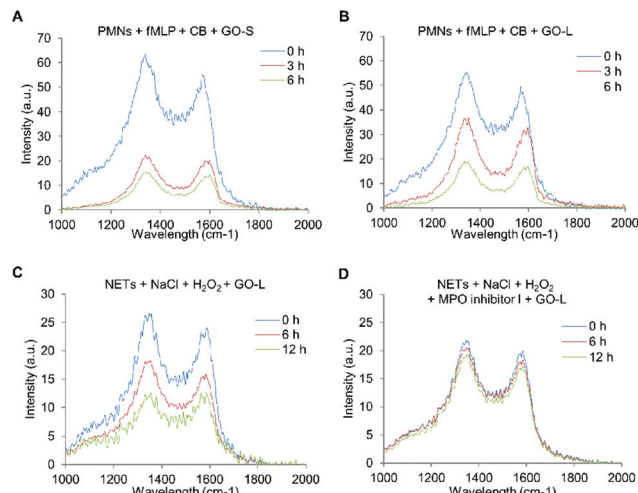


Fig. 5 Neutrophil degradation of GO. Freshly isolated human neutrophils were treated with fMLP (10 nM) and cytochalasin B (5 μ g mL⁻¹) to trigger degranulation and incubated with GO-S (a) or GO-L (b) for the indicated time-points. Raman confocal microscopic measurements showed biodegradation of GO-S and GO-L as determined by a reduction in the intensity of both the D and G band. The data shown represent an average of the whole scan (10 000 spectra per sample). Neutrophils were treated with 25 nM PMA for 3 h to trigger production of neutrophil extracellular traps (NETs). Then, NETs were purified and incubated with GO-L in the presence of NaCl and H₂O₂ for the indicated time-points and biodegradation was determined by Raman confocal microscopy. Degradation of GO was evidenced in the absence (c), but not in the presence (d) of MPO inhibitor-I (0.6 μ M), indicating that the degradation in NETs was MPO-dependent. The data represent an average of the whole scan (10 000 spectra per sample).

addition of H₂O₂ was required for MPO-dependent killing of *Staphylococcus aureus*.³² In line with these studies, we have shown that oxidized SWCNTs are degraded in NETs in the presence of H₂O₂.¹¹ We also demonstrated that purified NETs retained peroxidase activity up to 24 h and showed that this activity was abolished in the presence of MPO inhibitor-1.¹¹ Here we collected NETs produced upon phorbol 12-myristate 13-acetate (PMA) treatment of freshly isolated primary human neutrophils, and incubated the purified NETs with GO-L + H₂O₂ + NaCl, in the presence or absence of MPO inhibitor-1. Confocal Raman microspectrometric mapping clearly showed that both the D and G band intensities of GO were significantly reduced after 6 h and continued to decrease at 12 h of incubation with NETs in the presence of H₂O₂ (Fig. 5C). However, no reduction in the D and G band intensities was observed in the presence of MPO inhibitor-1 (Fig. 5D). This allowed us to conclude that the degradation of GO-L in NETs was mediated by MPO.

Degradation products of GO are not cyto- or genotoxic

While biodegradation of single-walled and multi-walled CNTs has been shown in several studies,³³ there is very little information on the potential toxicity of the degradation products. For graphene-based materials, there are no studies on the toxicity of degradation products following enzymatic degradation,

although a recent study showed that “aged” GO is non-cytotoxic.³⁴ Bai *et al.*¹⁵ provided insight into a potential mechanism of GO degradation *via* the photo-Fenton reaction and proposed, on the basis of several analytical techniques, that the degradation products may comprise of oxidized polycyclic aromatic hydrocarbons or PAHs. Here we monitored biodegradation of the small GO sheets (GO-S) by recombinant MPO in the presence of H₂O₂ and NaCl by using a matrix-assisted laser desorption-ionization time-of-flight (MALDI-TOF) instrument without any matrix. Instead, we used laser radiation that can be sufficiently absorbed by GO itself. GO and other analytes are then desorbed and ionized, creating an ion plume that is directed into the time-of-flight (TOF) analyzer. MALDI-TOF MS data of the 12 h degradation sample showed no presence of GO when compared to the parental sample (non-degraded GO) and the new peaks were not originally present in the MPO sample (ESI Fig. 2A†). The latter spectrum is shown only to rule out any small molecular weight components/impurities present in the MPO sample in the assignment of GO-related peaks or degradation products. MALDI-TOF MS spectra of GO samples undergoing degradation are shown in ESI Fig. 2B.† The spectrum obtained at the 0 h time-point revealed the presence of GO. From 3 h to 12 h, these peaks were no longer observed. However, the MALDI-TOF spectra of 0 h and 12 h degradation samples in *m/z* range from 100 to 500 were very similar and no significant new peaks were identified at 12 h of degradation; these peaks, therefore, cannot be attributed to GO degradation products (ESI Fig. 2C†). The assignment of specific molecular structures will require more in-depth mass spectrometry investigations. Nevertheless, the results are suggestive of enzymatic breakdown of GO-S, in accordance with the Raman, AFM, and TEM results reported in the preceding sections, with formation of (transient) degradation products of GO.

In order to investigate whether the degradation products of GO-S and GO-L could induce any loss of cell viability or DNA damage (genotoxicity) we exposed human BEAS-2B lung cells, which are considered a suitable model for *in vitro* studies of carcinogenesis,³⁵ for 24 h to the products of MPO-degraded GO-S and GO-L and to intact GO. H₂O₂ is known to exert DNA damage,³⁶ and we therefore eliminated the residual H₂O₂ potentially present in the reaction mixtures by adding catalase (ESI Fig. 3A†). DMSO was used as a positive control for cell death (Alamar blue assay), and the PAH, benzo[a]pyrene (B[a]P), a known carcinogen,³⁵ was used as a positive control for DNA damage (comet assay). The biodegradation products of GO did not trigger loss of cell viability (Fig. 6B) or DNA damage (Fig. 6C). We tested reaction mixtures (*i.e.*, GO-S or GO-L plus MPO + H₂O₂ + NaCl) obtained after incubation for 3, 6, 9, and 12 h in order to capture the effects not only of fully digested GO, but also those of the degradation products. In addition, we asked whether the degradation products generated upon incubation with MPO could bind to intact GO and thus become less bioavailable, thereby masking a genotoxic effect. To test this, using a model compound, we exposed cells to a mixture of B[a]P and intact GO. However, there was no

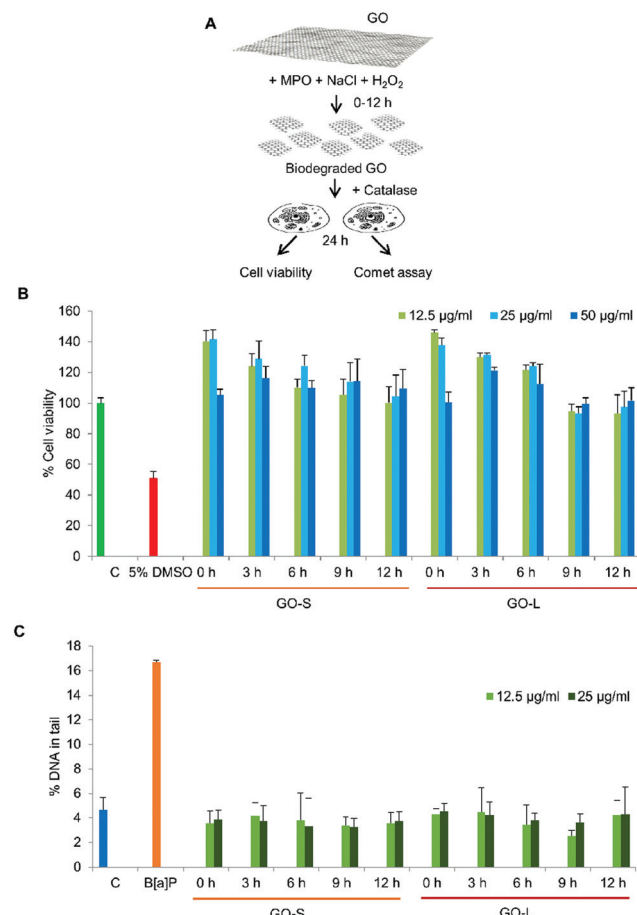


Fig. 6 GO degradation products are non-cytotoxic and non-genotoxic. (a) Large (GO-L) and small (GO-S) sheets were biodegraded by recombinant MPO in the presence of NaCl and H₂O₂ for 0–12 h, followed by treatment with catalase to quench the excess H₂O₂. Then, cell viability and genotoxicity assessment of the GO biodegradation products was performed using the human lung cell line BEAS-2B. (b) Cell viability was assessed by using the Alamar blue assay. No significant loss of cell viability was observed after exposure for 24 h of BEAS-2B cells with any of the reaction mixtures (intact or degraded GO). DMSO (5%) was used as a positive control. (c) The alkaline comet assay was performed to assess DNA damage. No significant increase of DNA in the comet tails was observed following exposure of BEAS-2B cells to the GO-S and GO-L biodegradation reaction mixtures. Benzo[a]pyrene (200 µM) was used as a positive control. Data shown in (b) and (c) are mean values ± S.D. of three independent experiments each performed in triplicates.

difference in genotoxicity, as determined by the alkaline comet assay, when cells were treated with B[a]P alone or in combination with GO-S or GO-L (ESI Fig. 3B†). The present results are in contrast to previous studies showing genotoxicity of intact GO *in vitro* and *in vivo* at high concentrations (400 µg mL⁻¹ and 4 mg per kg of body weight, respectively).^{37,38} Overall, our results revealed that neither GO nor the degradation products produced by enzymatic degradation of GO induced cytotoxicity or genotoxicity *in vitro* in human lung cells. This suggests that neutrophil-mediated degradation of GO, should this occur *in vivo*, will not give rise to genotoxic compounds.

Concluding remarks

In summary, we have shown that neutrophils are capable of mediating biodegradation of GO. Biodegradation is rapid (within hours) and occurs extracellularly when neutrophils are activated to undergo degranulation; we also showed that degradation occurs in neutrophil extracellular traps or NETs. GO degradation was shown to be MPO dependent, which is in line with previous work using the purified enzyme.¹² Importantly, the reaction mixtures of (partially) degraded GO were shown to be non-genotoxic using a human bronchial epithelial cell line (BEAS-2B) as a model. Understanding and controlling the interactions of GO with the immune system is of critical importance for any biomedical applications of GO.

Author contributions

S. P. M., A. G. and B. L. performed all the biological experiments, supervised by B. F. and K. B.; L. N. and A. F. R. characterized GO, supervised by K. K.; B. B. performed Raman analysis; M. F. performed AFM; C. V. performed TEM, supervised by M. T.; W. S. and P. M. F. performed the MALDI-TOF analysis, supervised by A. S.; all co-authors contributed to data analysis and interpretation; B. F. wrote the paper with S. P. M. and all co-authors approved the final version.

Conflicts of interest

The authors declare no competing financial interests.

Acknowledgements

This work was supported by the European Commission through the GRAPHENE Flagship Project (grant agreements no. 604391, and 696656) and the National Institute of Environmental Health Sciences (R01ES019304). We thank the University of Manchester Bioimaging Facility for the use of the TEM and AFM instruments for the characterization of GO.

References

- 1 A. C. Ferrari, F. Bonaccorso, V. Fal'ko, K. S. Novoselov, S. Roche, P. Bøggild, S. Borini, F. H. Koppens, V. Palermo, N. Pugno, J. A. Garrido, R. Sordan, A. Bianco, L. Ballerini, M. Prato, E. Lidorikis, J. Kivioja, C. Marinelli, T. Ryhänen, A. Morpurgo, J. N. Coleman, V. Nicolosi, L. Colombo, A. Fert, M. Garcia-Hernandez, A. Bachtold, G. F. Schneider, F. Guinea, C. Dekker, M. Barbone, Z. Sun, C. Gallois, A. N. Grigorenko, G. Konstantatos, A. Kis, M. Katsnelson, L. Vandersypen, A. Loiseau, V. Morandi, D. Neumaier, E. Treossi, V. Pellegrini, M. Polini, A. Tredicucci, G. M. Williams, B. H. Hong, J. H. Ahn, J. M. Kim, H. Zirath, B. J. van Wees, H. van der Zant, L. Occhipinti, A. Di Matteo, I. A. Kinloch, T. Seyller, E. Quesnel, X. Feng, K. Teo, N. Rupesinghe, P. Hakonen, S. R. Neil, Q. Tannock, T. Löfwander and J. Kinaret, Science and technology roadmap for graphene, related two-dimensional crystals, and hybrid systems, *Nanoscale*, 2015, 7(11), 4598–4810.
- 2 K. Bhattacharya, S. P. Mukherjee, A. Gallud, S. C. Burkert, S. Bistarelli, S. Bellucci, M. Bottini, A. Star and B. Fadeel, Biological interactions of carbon-based nanomaterials: from coronation to degradation, *Nanomedicine*, 2016, 12(2), 333–351.
- 3 D. Bitounis, H. Ali-Boucetta, B. H. Hong, D. H. Min and K. Kostarelos, Prospects and challenges of graphene in biomedical applications, *Adv. Mater.*, 2013, 25(16), 2258–2268.
- 4 C. Farrera and B. Fadeel, It takes two to tango: Understanding the interactions between engineered nanomaterials and the immune system, *Eur. J. Pharm. Biopharm.*, 2015, 95(Pt A), 3–12.
- 5 V. Brinkmann, U. Reichard, C. Goosmann, B. Fauler, Y. Uhlemann, D. S. Weiss, Y. Weinrauch and A. Zychlinsky, Neutrophil extracellular traps kill bacteria, *Science*, 2004, 303(5663), 1532–1535.
- 6 V. Papayannopoulos and A. Zychlinsky, NETs: a new strategy for using old weapons, *Trends Immunol.*, 2009, 30(11), 513–521.
- 7 P. Kruger, M. Saffarzadeh, A. N. Weber, N. Rieber, M. Radsak, H. von Bernuth, C. Benarafa, D. Roos, J. Skokowa and D. Hartl, Neutrophils: between host defence, immune modulation, and tissue injury, *PLoS Pathog.*, 2015, 11(3), e1004651.
- 8 M. B. Hampton, A. J. Kettle and C. C. Winterbourn, Inside the neutrophil phagosome: oxidants, myeloperoxidase, and bacterial killing, *Blood*, 1998, 92(9), 3007–3017.
- 9 V. E. Kagan, N. V. Konduru, W. Feng, B. L. Allen, J. Conroy, Y. Volkov, I. I. Vlasova, N. A. Belikova, N. Yanamala, A. Kapralov, Y. Y. Tyurina, J. Shi, E. R. Kisin, A. R. Murray, J. Franks, D. Stoltz, P. Gou, J. Klein-Seetharaman, B. Fadeel, A. Star and A. A. Shvedova, Carbon nanotubes degraded by neutrophil myeloperoxidase induce less pulmonary inflammation, *Nat. Nanotechnol.*, 2010, 5(5), 354–359.
- 10 A. A. Shvedova, A. A. Kapralov, W. H. Feng, E. R. Kisin, A. R. Murray, R. R. Mercer, C. M. St Croix, M. A. Lang, S. C. Watkins, N. V. Konduru, B. L. Allen, J. Conroy, G. P. Kotchey, B. M. Mohamed, A. D. Meade, Y. Volkov, A. Star, B. Fadeel and V. E. Kagan, Impaired clearance and enhanced pulmonary inflammatory/fibrotic response to carbon nanotubes in myeloperoxidase-deficient mice, *PLoS One*, 2012, 7(3), e30923.
- 11 C. Farrera, K. Bhattacharya, B. Lazzaretto, F. T. Andón, K. Hultenby, G. P. Kotchey, A. Star and B. Fadeel, Extracellular entrapment and degradation of single-walled carbon nanotubes, *Nanoscale*, 2014, 6(12), 6974–6983.
- 12 R. Kurapati, J. Russier, M. A. Squillaci, E. Treossi, C. Ménard-Moyon, A. E. Del Rio-Castillo, E. Vazquez, P. Samori, V. Palermo and A. Bianco, Dispersibility-dependent biodegradation of graphene oxide by myeloperoxidase, *Small*, 2015, 11(32), 3985–3994.

- 13 C. M. Girish, A. Sasidharan, G. S. Gowd, S. Nair and M. Koyakutty, Confocal Raman imaging study showing macrophage mediated biodegradation of graphene in vivo, *Adv. Healthcare Mater.*, 2013, **2**(11), 1489–1500.
- 14 B. L. Allen, G. P. Kotchey, Y. Chen, N. V. Yanamala, J. Klein-Seetharaman, V. E. Kagan and A. Star, Mechanistic investigations of horseradish peroxidase-catalyzed degradation of single-walled carbon nanotubes, *J. Am. Chem. Soc.*, 2009, **131**(47), 17194–17205.
- 15 H. Bai, W. Jiang, G. P. Kotchey, W. A. Saidi, B. J. Bythell, J. M. Jarvis, A. G. Marshall, R. A. Robinson and A. Star, Insight into the mechanism of graphene oxide degradation via the photo-Fenton reaction, *J. Phys. Chem. C*, 2014, **118**(19), 10519–10529.
- 16 S. Pan, N. P. Sardesai, H. Liu, D. Li and J. F. Rusling, Assessing DNA damage from enzyme-oxidized single-walled carbon nanotubes, *Toxicol. Res.*, 2013, **2**, 375–378.
- 17 H. Ali-Boucetta, D. Bitounis, R. Raveendran-Nair, A. Servant, J. Van den Bossche and K. Kostarelos, Purified graphene oxide dispersions lack in vitro cytotoxicity and in vivo pathogenicity, *Adv. Healthcare Mater.*, 2013, **2**(3), 433–441.
- 18 S. P. Mukherjee, N. Lozano, M. Kucki, A. E. Del Rio-Castillo, L. Newman, E. Vázquez, K. Kostarelos, P. Wick and B. Fadeel, Detection of endotoxin contamination of graphene based materials using the TNF- α expression test and guidelines for endotoxin-free graphene oxide production, *PLoS One*, 2016, **11**(11), e0166816.
- 19 S. P. Mukherjee, B. Lazzaretto, K. Hultenby, L. Newman, A. F. Rodrigues, N. Lozano, K. Kostarelos, P. Malmberg and B. Fadeel, Graphene oxide-induced plasma membrane changes in neutrophils revealed by time-of-flight secondary ion mass spectroscopy, *Chem*, 2018, [in press].
- 20 B. Fadeel, A. Åhlin, J.-I. Henter, S. Orrenius and M. B. Hampton, Involvement of caspases in neutrophil apoptosis: regulation by reactive oxygen species, *Blood*, 1998, **92**(12), 4808–4818.
- 21 K. Bhattacharya, C. Sacchetti, R. El-Sayed, A. Fornara, G. P. Kotchey, J. A. Gaugler, A. Star, M. Bottini and B. Fadeel, Enzymatic ‘stripping’ and degradation of PEGylated carbon nanotubes, *Nanoscale*, 2014, **6**(24), 14686–14690.
- 22 C. Farrera and B. Fadeel, Macrophage clearance of neutrophil extracellular traps is a silent process, *J. Immunol.*, 2013, **191**(5), 2647–2656.
- 23 F. T. Andón, A. A. Kapralov, N. Yanamala, W. Feng, A. Baygan, B. J. Chambers, K. Hultenby, F. Ye, M. S. Toprak, B. D. Brandner, A. Fornara, J. Klein-Seetharaman, G. P. Kotchey, A. Star, A. A. Shvedova, B. Fadeel and V. E. Kagan, Biodegradation of single-walled carbon nanotubes by eosinophil peroxidase, *Small*, 2013, **9**(16), 2721–2729.
- 24 K. J. Ong, T. J. MacCormack, R. J. Clark, J. D. Ede, V. A. Ortega, L. C. Felix, M. K. Dang, G. Ma, H. Fenniri, J. G. Veinot and G. G. Goss, Widespread nanoparticle-assay interference: implications for nanotoxicity testing, *PLoS One*, 2014, **9**(3), e90650.
- 25 E. Pieterse, N. Rother, C. Yanginlar, L. B. Hilbrands and J. van der Vlag, Neutrophils discriminate between lipopolysaccharides of different bacterial sources and selectively release neutrophil extracellular traps, *Front. Immunol.*, 2016, **7**, 484.
- 26 G. P. Kotchey, Y. Zhao, V. E. Kagan and A. Star, Peroxidase-mediated biodegradation of carbon nanotubes in vitro and in vivo, *Adv. Drug Delivery Rev.*, 2013, **65**(15), 1921–1932.
- 27 G. P. Kotchey, B. L. Allen, H. Vedala, N. Yanamala, A. A. Kapralov, Y. Y. Tyurina, J. Klein-Seetharaman, V. E. Kagan and A. Star, The enzymatic oxidation of graphene oxide, *ACS Nano*, 2011, **5**(3), 2098–2108.
- 28 N. Borregaard and J. B. Cowland, Granules of the human neutrophilic polymorphonuclear leukocyte, *Blood*, 1997, **89**(10), 3503–3521.
- 29 U. Gullberg, E. Andersson, D. Garwicz, A. Lindmark and I. Olsson, Biosynthesis, processing and sorting of neutrophil proteins: insight into neutrophil granule development, *Eur. J. Haematol.*, 1997, **58**(3), 137–153.
- 30 M. P. Fletcher and J. I. Gallin, Human neutrophils contain an intracellular pool of putative receptors for the chemoattractant N-formyl-methionyl-leucyl-phenylalanine, *Blood*, 1983, **62**(4), 792–799.
- 31 P. J. Honeycutt and J. E. Niedel, Cytochalasin B enhancement of the diacylglycerol response in formyl peptide-stimulated neutrophils, *J. Biol. Chem.*, 1986, **261**(34), 15900–15905.
- 32 H. Parker, A. M. Albrett, A. J. Kettle and C. C. Winterbourn, Myeloperoxidase associated with neutrophil extracellular traps is active and mediates bacterial killing in the presence of hydrogen peroxide, *J. Leukocyte Biol.*, 2012, **91**(3), 369–376.
- 33 G. P. Kotchey, S. A. Hasan, A. A. Kapralov, S. H. Ha, K. Kim, A. A. Shvedova, V. E. Kagan and A. Star, A natural vanishing act: the enzyme-catalyzed degradation of carbon nanomaterials, *Acc. Chem. Res.*, 2012, **45**(10), 1770–1781.
- 34 B. D. Holt, A. M. Arnold and S. A. Sydlik, In it for the long haul: the cytocompatibility of aged graphene oxide and its degradation products, *Adv. Healthcare Mater.*, 2016, **5**(23), 3056–3066.
- 35 B. van Agen, L. M. Maas, I. H. Zwingmann, F. J. Van Schooten and J. C. Kleinjans, B[a]P-DNA adduct formation and induction of human epithelial lung cell transformation, *Environ. Mol. Mutagen.*, 1997, **30**(3), 287–292.
- 36 H. L. Karlsson, A. R. Gliga, F. M. Calléja, C. S. Gonçalves, I. O. Wallinder, H. Vrieling, B. Fadeel and G. Hendriks, Mechanism-based genotoxicity screening of metal oxide nanoparticles using the ToxTracker panel of reporter cell lines, *Part. Fibre Toxicol.*, 2014, **11**, 41.
- 37 E. Hashemi, O. Akhavan, M. Shamsara, R. Rahighi, A. Esfandiar and A. R. Tayefeh, Cyto and genotoxicities of graphene oxide and reduced graphene oxide sheets on spermatozoa, *RSC Adv.*, 2014, **4**, 27213–27223.
- 38 O. Akhavan, E. Ghaderi, E. Hashemi and E. Akbari, Dose-dependent effects of nanoscale graphene oxide on reproduction capability of mammals, *Carbon*, 2015, **95**, 309–317.